PROTEINS
STRUCTURE ■ FUNCTION ■ BIOINFORMATICS

STRUCTURE NOTE

Induced conformational change in human IL-4 upon binding of a signal-neutralizing DARPin

Galina Obmolova,* Alexey Teplyakov, Thomas J. Malia, Edward Keough, Jinquan Luo, Raymond Sweet, Steven A. Jacobs, Fang Yi, Randi Hippensteel, Karyn T. O'Neil, and Gary L. Gilliland*

[1] Janssen Research & Development, LLC, Biotechnology Center of Excellence, Spring House, Pennsylvania, 19477

ABSTRACT

The crystal structure of DARPin 44C12V5 that neutralizes IL-4 signaling has been determined alone and bound to human IL-4. A significant conformational change occurs in the IL-4 upon DARPin binding. The DARPin binds to the face of IL-4 formed by the A and C α-helices. The structure of the DARPin remains virtually unchanged. The conformational changes in IL-4 include a reorientation of the C-helix Trp91 side chain and repositioning of CD-loop residue Leu96. Both side chains move by >9 Å, becoming buried in the central hydrophobic region of the IL-4:DARPin interface. This hydrophobic region is surrounded by a ring of hydrophilic interactions comprised of hydrogen bonds and salt bridges and represents a classical "hotspot." The structures also reveal how the DARPin neutralizes IL-4 signaling. Comparing the IL-4:DARPin complex structure with the structures of IL-4 bound to its receptors (Hage *et al.*, Cell 1999; 97, 271-281; La Porte *et al.*, Cell 2008, 132, 259-272), it is found that the DARPin binds to the same IL-4 face that interacts with the junction of the D1 and D2 domains of the IL-4Rα receptors. Signaling is blocked since IL-4 cannot bind to this receptor, which it must do first before initiating a productive receptor complex with either the IL-13α1 or the γ_c receptor.

Proteins 2015; 83:1191–1197.

Key words: DARPin; alternative scaffold; x-ray structure; IL-4:DARPin complex.

INTRODUCTION

Designed ankyrin repeat proteins (DARPins) are a promising class of nonimmunoglobulin proteins that can offer advantages over antibodies for target binding in drug discovery and drug development.[1,2] The basic ankyrin repeat module is composed of 33 amino acids structured as a β-turn followed by two antiparallel α-helices and a loop connected to the β-turn of the next repeat. The DARPin molecule is composed of a number of these linked ankyrin repeats sandwiched between the N- and C-terminal caps that bury the hydrophobic core of the terminal repeat segments. The repeats are stacked in the

Additional Supporting Information may be found in the online version of this article.

Abbreviations: DARPin, designed ankyrin repeat protein; DARPin_44, DARPin 44C12V5; IL-4, Interleukin-4; IL-13, Interleukin-13; MMS, microseed matrix screening.

*Correspondence to: Gary L. Gilliland, Ph.D., Biologics Research, Biotechnology Center of Excellence, Janssen Research & Development, LLC, 1400 McKean Road Spring House, PA 19477. E-mail:s ggillila@its.jnj.com (or) Galina Obmolova, Ph.D., Biologics Research, Biotechnology Center of Excellence, Janssen Research & Development, LLC, 1400 McKean Road Spring House, PA 19477. E-mail: gobmolov@its.jnj.com

Received 11 March 2015; Revised 8 April 2015; Accepted 11 April 2015

Raymond Sweet's current address is 700 Oak Springs Rd., Bryn Mawr, PA 19010

Randi Hippensteel's current address is Eurofins Lancaster Laboratories, 2425 New Holland Pike, Lancaster, PA 17601

Published online 21 April 2015 in Wiley Online Library (wileyonlinelibrary.com). DOI: 10.1002/prot.24815

molecule such that both the convex and concave surfaces are available for binding different types of targets.

In collaboration with Molecular Partners, DARPin 44C12V5 (DARPin_44) was developed to bind the human cytokine interleukin-4 (IL-4) with high affinity and block signaling through its receptors, IL-4Rα/IL-13Rα1 and IL-4Rα/γ_c. These receptors also bind the cytokine interleukin-13 (IL-13) in a manner similar to that observed for IL-4. Both cytokines are critical in the pathogenesis of airway hypersensitivity, mucus production, and airway remodeling in asthma.[3]

A large body of structural data exists for IL-4, which is an 11-kDa protein that folds into a 4-helical bundle. The data is comprised of the solution and crystal structures of IL-4 and a number of variants.[4–12] It, also, includes IL-4 interacting with its receptors.[13–15] The structures reveal a very consistent structure for the cytokine that undergoes very slight conformational changes upon binding to its receptors.

To get insight into the mechanism of action, the structure of DARPin_44 unbound and in complex with human IL-4 (IL-4:DARPin_44) have been determined at 1.9-Å and 2.0-Å, respectively. The structures and their comparison with themselves and with the structures of unbound IL-4, and the structures of the complexes with IL-4 and its receptor pairs IL-4Rα/IL-13Rα1 and IL-4Rα/γ_c was carried out revealing the mechanism of action and unexpectedly a significant conformational change in the IL-4 structure upon DARPin_44 binding.

MATERIALS AND METHODS

Protein production

Human IL-4 was expressed in *E. coli*, isolated from inclusion bodies and refolded (mtibio|Molecular Throughput). The protein (Lot 010512A) was received in 20 m*M* MES buffer, pH 6.0, 100 m*M* NaCl.

DARPin_44 was expressed in *E. coli* strain BL21 (DE3), purified by affinity (HisTrap), ion exchange and size exclusion chromatography.

Anti-il4 activity assay

HEK-Blue STAT-6 (Invivogen) cells were plated in 96-well cell culture plates at a density of 2.5×10^5/mL in 100 µL of cell culture media (DMEM + glucose) and incubated for 2 h. A dose response curve for the DARPin_44 was prepared (final starting concentration was 500 pM; 1:3 dilutions) and 50 µL was added to the plate. Subsequently, 50 µL of a 4× concentration of human IL-4 (final concentration of 1.6 pM (Peprotech) or 1.2 pM (R&D Systems)) was added to each well. Levels of SEAP (secreted embryonic alkaline phosphatase) were measured 24 h after treatment by the addition of 40 µL of supernatant to 160 µL of Quanti-Blue™ (Invivogen) in a clear 96-well plate. The plate was incubated for 40 min at 37 °C and absorbance (650 nm) was plotted as a function of DARPin_44 concentration to a sigmoidal dose response curve to determine IC_{50} values.

Complex preparation

The IL-4:DARPin_44 complex was prepared by mixing DARPin_44 with excess IL-4 at a molar ratio of 1:1.2, incubated for 2 h at 4 °C. The complex was then purified by size exclusion chromatography on a Superdex 200 (10/300) column (GE Healthcare) equilibrated in 20 m*M* HEPES pH 7.5, 250 m*M* NaCl. Fractions corresponding to the main peak were pooled, diluted with HEPES buffer to reduce the NaCl concentration, and EDTA was added to a final concentration 0.13 m*M*. The complex was concentrated using an Amicon-Ultra 5 kDa device to 10.7 mg/mL in 20 m*M* HEPES pH 7.5, 150 m*M* NaCl, 0.13 m*M* EDTA and used for crystallization.

Crystallization

DARPin_44

The DARPin_44 was concentrated to 38 mg/mL in 20 m*M* BIS TRIS buffer, pH 6.8, 250 m*M* NaCl. Crystallization was carried out by the vapor-diffusion method at 20 °C using a Mosquito robot (TTP Labtech) and an Oryx4 robot (Douglas Instruments). The experiments were composed of equal volumes of protein and reservoir solution in a sitting drop format in 96-well Corning 3550 plates. The initial screening was performed with the PEGs suite (Qiagen) and in-house screens. Intergrown crystal formations were obtained at different conditions. The seeds for microseed matrix screening (MMS)[16–18] were prepared from crystals, obtained at 25% PEG 1000 and 25% PEG 550 MME in 0.1*M* sodium acetate, pH 4.6. The MMS optimization was performed at 16 mg/mL protein concentration and resulted in crystals suitable for X-ray analysis. These grew from 22% PEG 3350, 0.2*M* $(NH_4)_2SO_4$, 3% isopropanol, and 3% dioxane.

IL-4:DARPin_44 complex

Crystallization of the IL-4:DARPin_44 complex was carried out by the vapor-diffusion method at 20 °C using a Mosquito robot (TTP Labtech). The experiments were composed of equal volumes of protein and reservoir solution in a sitting drop format in 96-well Corning 3550 plates. The screening was performed with the PEGs suite (Qiagen) and in-house screens. The crystals suitable for X-ray experiment were obtained from 18% PEG 3350, 0.2*M* lithium sulfate in 0.1*M* acetate buffer, pH 4.5.

X-ray data collection

DARPin_44

For X-ray data collection, one crystal was soaked for a few seconds in the mother liquor supplemented with

Table I
Crystal Data, X-ray Data, and Refinement Statistics

PDB code	DARPin_44 4YDW	IL-4:DARPin_44 4YDY
Crystal Data		
Space Group	$P2_12_12_1$	$P2_12_12_1$
Unit Cell Lengths (Å)	60.24,60.74,81.89	55.25, 113.66, 117.06
Molecules/ASU	2	2 complexes
V_m (Å^3/Da)	2.08	2.80
Solvent Content (%)	41	56
X-Ray Data		
Resolution (Å)	30-1.90 (1.95–1.90)	30–2.0 (2.05–2.00)
Measured Reflections	323,035 (11,000)	152,332 (10,222)
Unique Reflections	22,846 (1,258)	46,738 (3,246)
Completeness (%)	94.2 (71.5)	91.6 (86.5)
Redundancy	14.1 (8.7)	3.3 (3.1)
R_{merge} (I)	0.052 (0.294)	0.085 (0.338)
$<I/\sigma>$	43.5 (7.8)	10.6 (3.9)
B-factor(Wilson) (Å^2)	23.2	30.6
Refinement		
Reflections used in Refinement	21,630	45,618
Total No. Atoms	2,480	4,625
No. Water Molecules	170	364
R-factor	0.170	0.202
R-free	0.212	0.239
rmsd Bond Lengths (Å)	0.007	0.008
rmsd Bond Angles (°)	1.117	1.0
Mean B-factor (Å^2)	19.3	34.4

20% glycerol and was frozen in the stream of nitrogen at 100 K. Diffraction data were collected using a Rigaku MicroMax^{TM}-007HF microfocus X-ray generator equipped with a Saturn 944 CCD detector over a 360° crystal rotation with 2-min exposures per 0.25°-image and were processed with the program XDS.[19]

IL-4:DARPin_44 complex

For X-ray data collection, one crystal was soaked for a few seconds in the mother liquor supplemented with 18% glycerol and was frozen in liquid nitrogen. Diffraction data were collected at the IMCA beamline 17-ID at the Advanced Photon Source (Argonne, IL) at 100 K over a 90° crystal rotation with 0.5-s exposures per 0.5°-image and were processed with the program XDS.[19]

Structure determination

The structures of DARPin_44 and the IL-4:DARPin_44 complex were both solved by molecular replacement. For the complex structure the crystal structures of a DARPin specific for IL-13 (unpublished data) and human IL-4 (**2b8u**)[12] were used as search models, and for the DARPin_44 alone, the DARPin_44 structure from the IL-4 complex was used as a search model. All crystallographic calculations were performed with the CCP4 suite of programs.[20] Model adjustments were carried out using the program COOT.[21] Figures involving the structures were made with PyMOL Molecular Graphics System, Version 1.4.1 (Schrödinger, LLC). The superpositioning of the structures was carried out using the CCP4 program SUPERPOSE.[22] The final refinement statistics are given in Table I. The atomic coordinates and structure factors have been deposited in the Protein Data Bank with PDB ids **4ydw** and **4ydy** for DARPin_44 and the IL-4:DARPin_44 complex, respectively.

RESULTS

Neutralization of IL-4 signaling by binding to DARPin_44

DARPin_44 was selected for its ability to bind to recombinant human IL-4 with high affinity and to neutralize IL-4 signaling. A detailed description of the selection of this molecule from the DARPin library will be described in future publications. Binding of IL-4 to IL-4Rα/IL-13Rα1 and IL-4Rα/γ_c results in downstream phosphorylation of the transcriptional activator STAT6. Supporting Information Figure S1 demonstrates blockade of IL-4 induced secretion of alkaline phosphatase by DARPin_44 in a reporter cell line in which alkaline phosphatase expression is driven by a STAT6 signaling. In this assay, DARPin_44 potently neutralizes the activity of recombinant human IL-4 with an IC_{50} of 5 pM. The IC_{50} obtained in this assay is in close agreement with the binding constant of DARPin_44/IL-4 interactions measured to be 10 pM by surface plasmon resonance (data not shown).

DARPin_44 and IL-4:DARPin_44 complex structures

The structure of the DARPin_44 has been determined at 1.9-Å resolution. Two copies of the DARPin_44 are present in the asymmetric unit (designated as chain A and B). The structures of the two chains are for the most part well-ordered and very similar (rmsd of 0.26 Å), but the first 12 amino acid residues at the N-terminus are missing in both chains. For chain B residue 169 is also disordered. Side chains of Asp13 and Asn169 for chain A and Asp13 and Leu168 for chain B are also partially disordered. The conformations of the side chains of the hydrophobic core residues are well conserved. Surface residues side-chain conformations, in particular Lys, Arg, Glu and Asp, vary considerably. A number of the changes are a result of the differences in the crystal packing interactions between the two copies of the DARPin_44 in the asymmetric unit.

The IL-4:DARPin_44 complex structure has been determined at 2.0-Å resolution [Fig. 1(A)]. The asymmetric unit of the crystal contains two copies of the complex, which is comprised of chains I/A and J/B for the IL-4:DARPin_44 components, respectively. The complete sequences of the IL-4 and the DARPin_44 constructs crystallized in the complex are shown in Supporting Information Figure S2. In the structure, the first 11 N-terminal amino acid residues and the C-terminal residue (169) in

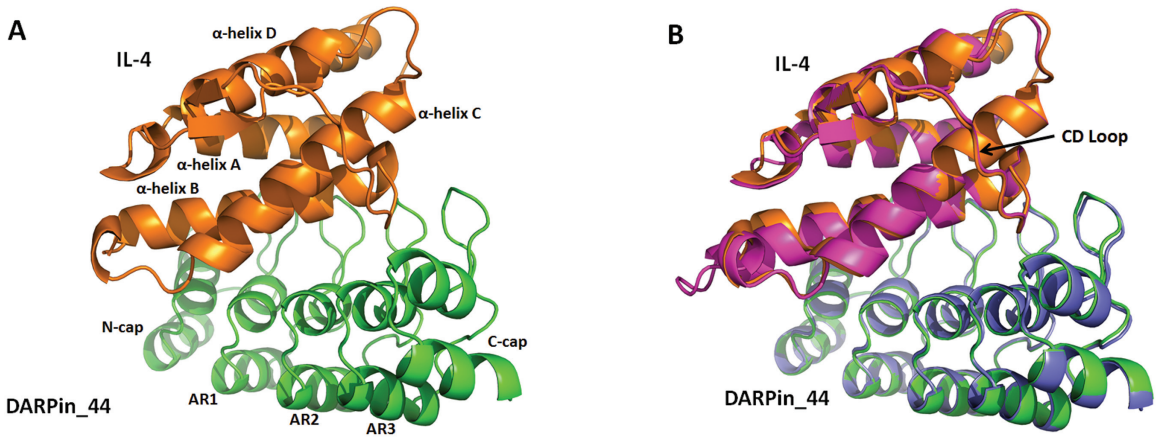

Figure 1

Cartoon representations of the structure of the IL-4:DARPin_44 complex: (**A**) the IL-4 molecule (chain I) is shown in orange and the DARPin_44 (chain A) shown in green. **B**: The superposition of the two copies of the IL-4:DARPin_44 complex found in the crystallographic asymmetric unit (the A/I and B/J chain pairs are shown in orange/green and magenta/violet, respectively).

both of the two DARPin_44s (chains A and B) are disordered and are not visible in the electron density map. The backbone atoms for the two DARPin_44 chains A and B are clearly visible in the electron density map, but side chain atoms for residues 12–13 and residue 12 for chains A and B, respectively, are not visible. The two copies of IL-4 also have missing residues due to disorder, residues 67–72 for chain I and the first two N-terminal residues (1-2) and the last 3 C-terminal residues (127–129) for chain J. The number of disordered or partially disordered side chains is larger in the IL-4 molecules than that observed for the DARPin_44s. These include residues 1–2, 21–23, 26, 37–38, 61, 63–64, 66, 73, 75, and 129 for chain I and residues 3, 21, 23, 26, 36, 69, 71–72 and 75. These are primarily surface residues that are not involved in the binding interaction with the DARPin_44. Associated with the two complexes are 364 water molecules. In addition, two glycerol molecules are bound on the surface of DARPin_44 A, and an acetate ion is bound to DARPin_44 B.

The structural comparison of the two copies of the IL-4:DARPin_44 complexes reveals deviations in the two structures as expected [see Fig. 1(B)]. An RMSD of 0.75 Å is observed (for 275 Cα's from both the IL-4 and the DARPin_44. Interestingly, in the comparison of the two DARPin_44 molecules an RMSD of 0.28 Å is observed for 157 Cα positions, while an RMSD of 0.89 Å is observed for 118 Cα positions of the two copies of IL-4. Thus, the IL-4 structural differences have the largest influence on the RMSD for the entire complex.

IL-4:DARPin binding interactions

The DARPin_44 binding in the complex is centered on the C-terminal end of the IL-4 C α-helix and the CD loop that connects the C helix with the D helix. Two other IL-4 α-helices, A and B, participate in the binding interaction, with the A helix participating much more than the B helix. Only two or three residues for the I and J chains of the B helix have contacts with DARPin_44. The C-terminus of the C helix binds in the groove on the concave surface near the C-terminal region of DARPin_44 and the A and B helices flank the C helix.

The binding interactions between DARPin_44 and IL-4 are characterized by a ring of hydrophilic interactions comprised of hydrogen bonds and salt-bridges surrounding a central region predominated by hydrophobic interactions. The buried surface areas of the IL-4:DARPin_44 complex are 1150 and 1130 $Å^2$ for the A and B DARPin_44 chains, and 1120 $Å^2$ for both the I and J chains of the IL-4s. The extent of this area is consistent for other high affinity protein:protein binding interactions.[23] The K_D for DARPin_44 binding to IL-4 is 13-21 pM as measured by SPR (unpublished data).

The details of the interactions between the DARPin_44 and the IL-4 are illustrated in Supporting Information Figure S3. A number of conserved electrostatic interactions are observed between the two pairs of binding partners (A/I and B/J). These include three salt bridge pairs for the IL-4:DARPin_44 complex: Asp45:Lys12; Glu56:Arg88; and Arg78:Glu8. The B/J pair has one additional salt bridge involving Asp57:Arg81. Approximately one dozen conserved hydrogen bonds are observed between amino acid residues of the two chains in the two complexes, but because of packing differences the A/I pair has 5 and the B/J pair has 6 additional hydrogen bonds. These interactions surround the hydrophobic core region.

The hydrophobic interactions between DARPin_44 and IL-4 center around 2 residues, Trp91 and Leu96, of IL-4. The DARPin_44 residues that interact with IL-4 Trp91 include Asp81, Phe89, Asp110, Ala112, Val114,

Val119, Tyr 123, and Phe145. A conserved hydrogen bond (in both copies of the complex) is observed between IL-4 Trp91 NE1 and DARPin_44 Tyr123 OH. The residues interacting with IL-4 Leu96 are Val114, His118, Phe122, Tyr123 and Ile152. These interactions are completely conserved between both binding pairs in the asymmetric unit. It should be noted that only two DARPin_44 residues, Val114 and Tyr123, interact with both of the IL-4 residues.

IL-4 conformational changes induced upon darpin_44 binding

A significant conformational change in IL-4 is observed with DARPin_44 binding to IL-4 at the C-terminus of the C α-helix and in the N-terminal region of the CD loop (shown in Fig. 2). The structure of this region is well defined in the electron density map (shown in Supporting Information Figure S4). Nearly identical conformation changes are observed in both the I and J chains in the asymmetric unit, which points to DARPin_44-binding induced changes in the IL-4 molecule rather than an influence of crystal packing. In contrast, the DARPin_44, in the region that interacts with IL-4, has no significant conformational changes. A few DARPin_44 side chains move slightly, but overall the binding region of the DARPin_44 in the complex is very similar to that observed in the unbound state.

The two IL-4 molecules in the asymmetric unit, the I and J chains, have an rmsd of 0.36 Å and, as mentioned above, have the same conformational changes relative to the unbound IL-4 (**2b8u**).[12] Three IL-4 amino acid residues, Arg53, Trp91 and Leu96 play key roles in the observed changes. The C-terminal region of the C-helix becomes distorted from the classical α-helical geometry, which is the result of the side chain of Trp91 rotating 180° from the rotamer observed in the unbound IL-4 structure (**2b8u**)[12] and become buried in the hydrophobic core of the IL-4:DARPin_44 binding interface. The movement of the side chain is quite dramatic with the CZE atom of the six-membered ring moving by >10 Å, and the backbone CA moves by nearly 2.5 Å. One consequence of this change in rotamer, is that the IL-4 Arg53 side chain that occupies the space where the Trp91 side chain has to alter its position. The Arg53 CZ atom moves by >5.0 Å, while the backbone atom position remain unchanged. The new position of the Trp91 side chain interacts primarily through hydrophobic interactions with the DARPin_44 and through a hydrogen bond with DARPin_44 Tyr123 as described earlier.

The third IL-4 amino acid residue, Leu96, undergoes the most significant structural reorganization compared to that observed for Trp91 and Arg53. This residue is located in the N-terminal region of the loop that connects the C and D α-helices. The Leu96 side chain flips from its observed location in **2b8u** to bury itself in the hydrophobic core of the IL-4:DARPin_44 binding interface. The CG atom of the side chain moves a distance > 9.0 Å, and the CA atom moves by almost 5 Å. The backbone of this region of the CD loop begins diverging from that observed in the unbound IL-4 at residue 95, has a maximum deviation at residue Leu96 and then converges at residue Glu103. This change in backbone and the reorientation of Leu96 allows the side chain to bury in the hydrophobic core of the IL-4:DARPin_44 binding interface. The interactions of the Leu96 side chain with the DARPin_44 amino acid residues are described above.

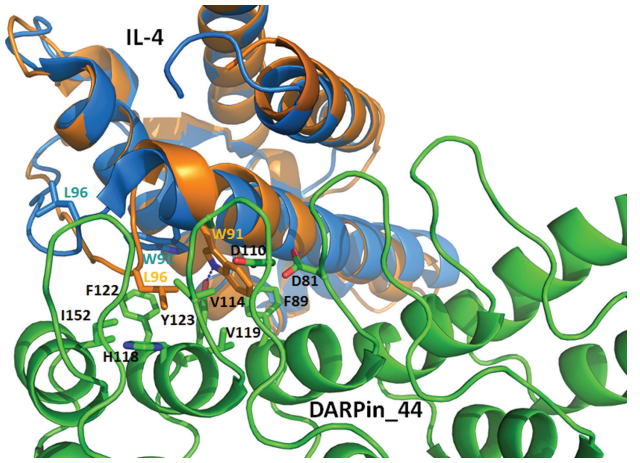

Figure 2

The structure of unbound IL-4 (marine blue) (**2b8u**)[12] superimposed on the IL-4:DARPin_44 complex (orange and green) illustrating the conformational change in IL-4 observed when bound to DARPin_44. The side chains of the two IL-4 residues Trp91 and Leu96 are shown as stick figures. The DARPin_44 residues that interact with these two hydrophobic residues are also shown as stick figures. The hydrogen bond between the IL-4 Trp91 NE1 and DARPin_44 Tyr44 OH is shown with a dashed line.

Comparison of IL-4 binding to receptor and to DARPin_44

As mentioned in the introduction, IL-4 signaling can be accomplished by its interaction with two different pairs of receptors, IL-4Rα and γ_c (type I interaction) or IL-4Rα and IL-13Rα1 (type II interaction).[13] Structures of these complexes (IL-4 bound to both receptor pairs, 2.9-Å and 3.0-Å resolution, respectively)[13] and IL-4 bound to IL-4Rα (2.3-Å resolution)[15] allow the determination of how DARPin_44 binding to IL-4 inhibits signaling. The DARPin_44 binds to the A and C α-helices of IL-4 in the same region that is involved in IL-4's binding to IL-4Rα that interacts with the junction of the D1 and D2 domains [see Fig. 3(A,B)].

The specific interactions of IL-4 and the DARPin_44 are somewhat similar to that found in the IL-4 and

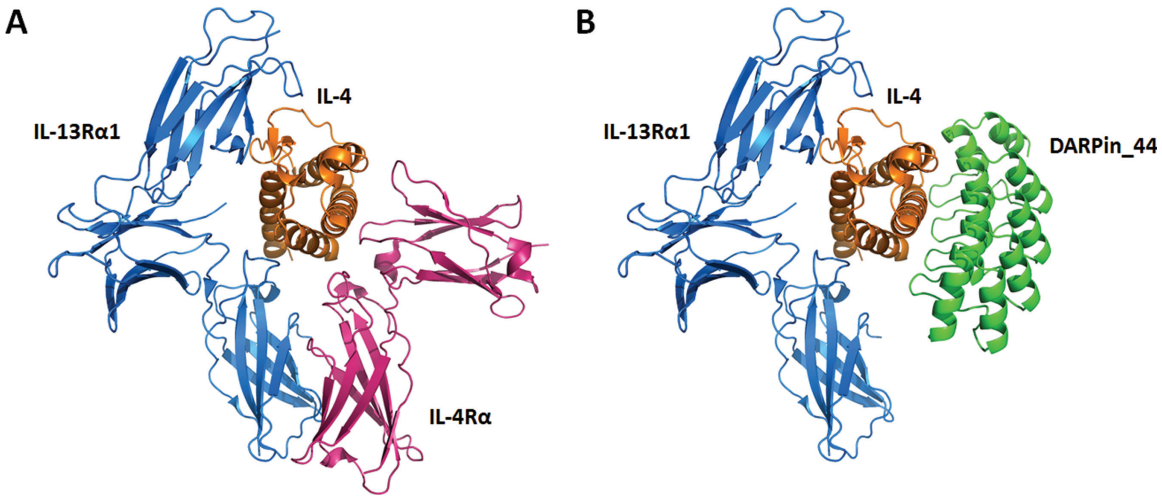

Figure 3

The structural comparison of the IL-4:DARPin_44 complex with the IL-4Rα–IL-13Rα1:IL-4 complex (**3 bpn**).[13] **A**: The IL-4Rα, IL-13Rα1, and IL-4 signaling complex are shown in magenta, blue, and orange, respectively. **B**: DARPin_44 (green) is shown bound to IL-4 (orange). Binding of DARPin_44 to IL-4 sterically occludes the IL-4Rα binding, but it does not block IL-4's binding to IL-13α1 (blue).

IL-4Rα interaction. The salt bridge between IL-4 Arg88 and the DARPin_44 Glu56 that mimics one observed in the receptor complex between IL-4 Arg88 and the receptor Asp72. Other polar interactions in the receptor complex include interactions between Arg88 and Glu9 of the DARPin_44 and receptor residues Tyr13, Ser70, and Tyr183. Interestingly, in the IL-4:IL-4Rα complex, the hydrophilic interactions are found at the center of the interaction surface with hydrophobic interactions on the periphery. This is inverted compared to what is observed in the IL-4:DARPin_44 interactions, which has hydrophobic residues centrally located with hydrophilic interactions on the periphery.

DISCUSSION

The IL-4:DARPin_44 interaction represents a classic "hot spot" interaction.[23,24] In such interactions, different binding-site residues contribute differently to the energetics of binding. Three amino acid residues, tryptophan, tyrosine, and arginine are the most prevalent in hot spots. As mentioned above, the IL-4:DARPin_44 interface is comprised of a hydrophobic patch surrounded by a ring of hydrophilic residues engaged in hydrogen bonds. Interestingly, one of the key interactions at the center of the interface is hydrogen bond between IL-4 Tyr91 NE1 and the DARPin_44 Tyr123 OH.

Two important findings have resulted from the analysis of the IL-4:DARPin-44 complex and its comparison with other IL-4 structures and its complex with its receptors. First, the structure of the complex provides a rationale of how DARPin_44 binding disrupts IL-4 signaling through both of its receptor complexes comprised of IL-4Rα with IL-13Rα1 or γ_c. Second, it reveals an unexpected and significant conformational change in the IL-4 structure upon DARPin-44 binding.

Regarding the first point, IL-4 must bind the IL-4Rα receptor first before binding to the second receptor, IL-13Rα1 or γ_c, occurs.[13,25] The IL-4Rα receptor binds to the C and D α-helices of IL-4, which is also where the DARPin_44 binds. Thus, the DARPin_44, with a higher binding affinity (13-21 pM) for IL-4 than the IL-4Rα receptor (1 nM)[13] binds to IL-4 and sterically blocks its interaction with the receptor. Thus, signaling is blocked, since neither of the receptor pairs can form the signaling complex.

With respect to the second point, as detailed above, the C α-helix and the N-terminal region of the CD loop that connects the C and D α-helices undergo a conformational change burying IL-4's Trp91 (with a reposition of the Arg53 side chain) and Leu96 side chains in a hydrophobic pocket in the center of the IL-4:DARPin_44 binding interface. A comparison with X-ray and NMR structures of unbound IL-4 structures[4–12,26] and those bound to one or more receptor chain (ECDs)[13–15] with the IL-4 bound to DARPin_44 in the complex finds no comparable conformational change. Thus, the DARPin_44 binding to IL-4 is responsible for the changes observed. The argument for this is strengthened since these changes are observed in both copies of the complex in the asymmetric unit.

The results of the study presented here provide an interesting example in which a very stable high-affinity DARPin binds to a cytokine with a well characterized

structure, inducing a quite significant change in the conformation of the IL-4 C α-helix and the CD loop region. It can be argued here that the DARPin binding is a dynamic event that induces the structural changes observed in the IL-4, changes that are not usually observed in the structure as evident in both the crystal and solution structures of the cytokine that have been determined.

REFERENCES

1. Binz HK, Amstutz P, Kohl A, Stumpp MT, Briand C, Forrer P, Grutter MG, Pluckthun A. High-affinity binders selected from designed ankyrin repeat protein libraries. Nat Biotechnol 2004;22: 575–582.
2. Seeger MA, Zbinden R, Flutsch A, Gutte PG, Engeler S, Roschitzki-Voser H, Grutter MG. Design, construction, and characterization of a second-generation DARP in library with reduced hydrophobicity. Protein Sci 2013;22:1239–1257.
3. Van Dyken SJ, Locksley RM. Interleukin-4- and interleukin-13-mediated alternatively activated macrophages: roles in homeostasis and disease. Annu Rev Immunol 2013;31:317–343.
4. Powers R, Garrett DS, March CJ, Frieden EA, Gronenborn AM, Clore GM. Three-dimensional solution structure of human interleukin-4 by multidimensional heteronuclear magnetic resonance spectroscopy. Science 1992;256:1673–1677.
5. Powers R, Garrett DS, March CJ, Frieden EA, Gronenborn AM, Clore GM. The high-resolution, three-dimensional solution structure of human interleukin-4 determined by multidimensional heteronuclear magnetic resonance spectroscopy. Biochemistry 1993;32: 6744–6762.
6. Muller T, Dieckmann T, Sebald W, Oschkinat H. Aspects of receptor binding and signalling of interleukin-4 investigated by site-directed mutagenesis and NMR spectroscopy. J Mol Biol 1994;237:423–436.
7. Muller T, Oehlenschlager F, Buehner M. Human interleukin-4 and variant R88Q: phasing X-ray diffraction data by molecular replacement using X-ray and nuclear magnetic resonance models. J Mol Biol 1995;247:360–372.
8. Smith LJ, Redfield C, Boyd J, Lawrence GM, Edwards RG, Smith RA, Dobson CM. Human interleukin 4. The solution structure of a four-helix bundle protein. J Mol Biol 1992;224:899–904.
9. Hulsmeyer M, Scheufler C, Dreyer MK. Structure of interleukin 4 mutant E9A suggests polar steering in receptor-complex formation. Acta Crystallogr D Biol Crystallogr 2001;57(Pt 9):1334–1336.
10. Wlodawer A, Pavlovsky A, Gustchina A. Crystal structure of human recombinant interleukin-4 at 2.25 a resolution. FEBS Lett 1992;309: 59–64.
11. Walter MR, Cook WJ, Zhao BG, Cameron RP Jr., Ealick SE, Walter RL Jr., Reichert P, Nagabhushan TL, Trotta PP, Bugg CE. Crystal structure of recombinant human interleukin-4. J Biol Chem 1992; 267:20371–20376.
12. Kraich M, Klein M, Patino E, Harrer H, Nickel J, Sebald W, Mueller TD. A modular interface of IL-4 allows for scalable affinity without affecting specificity for the IL-4 receptor. BMC Biol 2006;4:13
13. LaPorte SL, Juo ZS, Vaclavikova J, Colf LA, Qi X, Heller NM, Keegan AD, Garcia KC. Molecular and structural basis of cytokine receptor pleiotropy in the interleukin-4/13 system. Cell 2008;132: 259–272.
14. Junttila IS, Creusot RJ, Moraga I, Bates DL, Wong MT, Alonso MN, Suhoski MM, Lupardus P, Meier-Schellersheim M, Engleman EG, Utz PJ, Fathman CG, Paul WE, Garcia KC. Redirecting cell-type specific cytokine responses with engineered interleukin-4 superkines. Nat Chem Biol 2012;8:990–998.
15. Hage T, Sebald W, Reinemer P. Crystal structure of the interleukin-4/receptor alpha chain complex reveals a mosaic binding interface. Cell 1999;97:271–281.
16. Ireton GC, Stoddard BL. Microseed matrix screening to improve crystals of yeast cytosine deaminase. Acta Crystallogr D Biol Crystallogr 2004;60(Pt 3):601–605.
17. D'Arcy A, Villard F, Marsh M. An automated microseed matrix-screening method for protein crystallization. Acta Crystallogr D Biol Crystallogr 2007;63(Pt 4):550–554.
18. Obmolova G, Malia TJ, Teplyakov A, Sweet R, Gilliland GL. Promoting crystallization of antibody-antigen complexes via microseed matrix screening. Acta Crystallogr D Biol Crystallogr 2010;66(Pt 8): 927–933.
19. Kabsch W. XDS. Acta Crystallogr D Biol Crystallogr 2010;66(Pt 2): 125–132.
20. Collaborative Computational Project Number 4. The CCP4 suite: programs for protein crystallography. Acta Crystallogr D Biol Crystallogr 1994;53:240–255
21. Emsley P, Lohkamp B, Scott WG, Cowtan K. Features and development of coot. Acta Crystallogr D Biol Crystallogr 2010;66(Pt 4): 486–501.
22. Krissinel E, Henrick K. Secondary-structure matching (SSM), a new tool for fast protein structure alignment in three dimensions. Acta Crystallogr D Biol Crystallogr 2004;60(Pt 12-1):2256–2268.
23. Bogan AA, Thorn KS. Anatomy of hot spots in protein interfaces. J Mol Biol 1998;280:1–9.
24. Li J, Liu Q. 'Double water exclusion': a hypothesis refining the O-ring theory for the hot spots at protein interfaces. Bioinformatics 2009;25:743–750.
25. Andrews AL, Holloway JW, Puddicombe SM, Holgate ST, Davies DE. Kinetic analysis of the interleukin-13 receptor complex. J Biol Chem 2002;277:46073–46078.
26. Redfield C, Smith LJ, Boyd J, Lawrence GM, Edwards RG, Gershater CJ, Smith RA, Dobson CM. Analysis of the solution structure of human interleukin-4 determined by heteronuclear three-dimensional nuclear magnetic resonance techniques. J Mol Biol 1994;238:23–41.